Characteristics of cloud-to-ground (CG) lightning and differences between +CG and -CG in China regarding CNLDN network

Ruijiao Jiang[a], Guoping Zhang[a,*], Shudong Wang[a], Bing Xue[a], Zhengshuai Xie[b], Tingzhao Yu[a], Kuoyin Wang[a], Jin Ding[a], Xiaoxiang Zhu[a]

[a] Public Meteorological Service Center, China Meteorological Administration, Beijing 100081, China

[b] Weather Modification Centre, China Meteorological Administration, Beijing 100081, China

[*] Corresponding author. E-mail address: zhanggp@cma.gov.cn

Abstract

The lightning location system consisting of multiple ground-based stations is an effective means of lightning observation. The dataset from CNLDN (China National Lightning Detection Network) in 2016-2021 is employed to analyze the temporal and spatial lightning distributions and the differences between +CG (cloud-to-ground lightning) and -CG flashes in China. On the monthly scale, lightning activity is most prevalent during the summer months (June, July, and August), accounting for 70.7% of the year. Spring sees more lightning than autumn, and winter has only a small amount in southeastern coastal areas. During the day, the frequency of lightning peaks at 15:00-17:00 CNT and is lowest at 8:00-11:00 CNT. For the period with high CG frequency (summer of a year or afternoon of a day), the proportion of +CG flashes and the discharge intensity is relatively small. Winter in a year and morning or midnight in a day correspond to a greater +CG proportion and discharge current. Spatially, low latitude, undulating terrain, seaside, and humid surface are favorable factors for lightning occurrence. Thus, the southeast coastland has the largest lightning density, while the northwest deserts and basins and the western and northern Tibetan Plateau with altitudes over 6000 meters have almost no lightning. The proportion of +CG flashes and the discharge intensity are low in the southern region with high lightning density but diverse in other regions. The Tibetan Plateau leads to the complexity of lightning activity in China and lays the foundation for studying the impact of surface elevation on lightning. Results indicate that the +CG ratio on the eastern and southern Tibetan Plateau is up to 15%, larger than the plain regions. The current of -CG is positively correlated with altitude, but +CG shows a negative correlation, resulting in a large difference in current between +CG and -CG on the plain and approach on the plateau.

Keywords: China, CNLDN, Lightning characteristics, +CG flashes, Current peak

value

1. Introduction

Most lightning is generated mainly through meso-small scale severe convective weather, with few occurring in stratus clouds and tropical cyclones and occasionally during volcanic eruptions, nuclear explosions, and dust storms (Rakov and Uman, 2003). Lightning, a violent long-distance transient discharge phenomenon, could cause severe disasters such as human and animal casualties, forest fires, and electronic and communication equipment interruptions. Lightning is also associated with extreme weather events such as heavy rainfall, hail, and strong winds. These events can cause damage to infrastructure, crops and property, and pose a threat to public safety. Therefore, advanced lightning monitoring technology is necessary for the development of lightning science and also scientific protection against meteorological disasters.

Lightning discharge emits electromagnetic spectrums with a broad range, providing an essential avenue for lightning detection. The very low frequency / low frequency (VLF/LF, 20-300 kHz) band radiation is mainly produced by the cloud-to-ground (CG) return strokes, intracloud (IC) K-changes, and other discharge processes with a large spatial scale(Preston and Tolver, 1989; Schulz et al., 2016; Cummins et al., 1998). VLF/LF electromagnetic waves could propagate along the ground surface or be reflected between the surface and ionosphere propagation, with the superiority of long propagation distance (hundreds to thousands of kilometers) and slow attenuation. This frequency range thus is suitable for large-scale lightning detection and is currently the most commonly used target detection band for ground-based lightning location systems(Wang et al., 2020).

Representative examples of modern lightning location systems working in VLF/LF band are mainly the U.S. National Lightning Detection Network (NLDN), Los Alamos Sferic Array (LASA), European Cooperation for Lightning Detection (EUCLID), etc. The three nationwide detection networks in China are China National Lightning Detection Network (CNLDN), operated by the Meteorological Observation Centre of China Meteorological Administration (CMA), the Lightning Location System (LLS) of the State Grid Corporation of China, and the Three-Dimensional Lightning Location System (3D-LLS) deployed by the Institute of Electrical Engineering of Chinese Academy of Sciences (CAS). There are also small-scale and refined detection systems in local China areas, such as the Beijing Lightning Network (BLNET) established by the Institute of Atmospheric Physics of CAS, the Guangdong-Hongkong-Macao Lightning Location System (GHMLLS) deployed by the meteorological departments of Guangdong Province, Hongkong, and Macao.

China spans a wide range of latitudes from north to south and significant terrain changes from east to west. The western and northern parts of the Tibetan Plateau have large uninhabited areas with altitudes above 4500 m. The above factors pose challenges for the installation of lightning detectors and the improvement of the accuracy of

locating algorithms. Currently, most of the analyses of lightning characteristics in China are based on lightning imagers on satellites and the World-Wide Lightning Location Network (WWLLN)(Ma et al., 2005; You et al., 2019; Ma et al., 2021). However, the Optical Transient Detector (OTD) on Microlab-1 and Lightning Imaging Sensor (LIS) on TRMM was no longer updated, and the Chinese Lightning Mapping Imager (LMI) on FY-4A is not oriented to the China area all year round. Meanwhile, the detection rate of the satellite sensor and WWLLN is low and not valuable for analyzing the difference between different types of flashes. CNLDN is nowadays the most widely used system by the meteorological departments in China and has accumulated observational data for many years. Lightning studies based on CNLDN data are currently relatively limited and generally focus on localized areas(Liu et al., 2021; Li et al., 2020).

This study makes use of CNLDN data from 2016-2021 to analyze the lightning climate over China by dividing the continental region into four blocks. We also focus on comparing the differences between +CG and -CG flashes regarding temporal and spatial distribution. In addition, China's wide latitude and longitude range and complex topography make for our studying the relationship between lightning and geographic factors.

2. Data source

CNLDN was initially developed in 2007 by the National Space Science Center (NSSC) of CAS and is now operated by the Meteorological Observation Centre of CMA. The system comprised 435 sub-stations (as of 2020), each equipped with a lightning detector, and a central data processing station located at the National Meteorological Information Center. Although with some blind areas in Xinjiang and Xizang, CNLDN can generally achieve nationwide lightning detection. The distribution of sub-stations can be seen in Fig. 1.

The network uses a time-of-arrival (TOA) technique, with a GPS timing error of fewer than 20 ns (in clear sky conditions), to detect VLF/LF pulses of CG return strokes. A lightning flash may consist of several CG strokes, and the system groups single-point signals to a flash event based on their separation in time and space. Return strokes within a 500 ms time interval and 10 km distance interval are classified as a single CG flash, with the first detected stroke representing the entire flash.

In this study, we analyze lightning characteristics in inland China using the CNLDN dataset from 2016-2021, downloaded from the CMA big data cloud platform. For each flash, we can obtain information on the time of occurrence, latitude, longitude, current peak value, and the number of triggered stations.

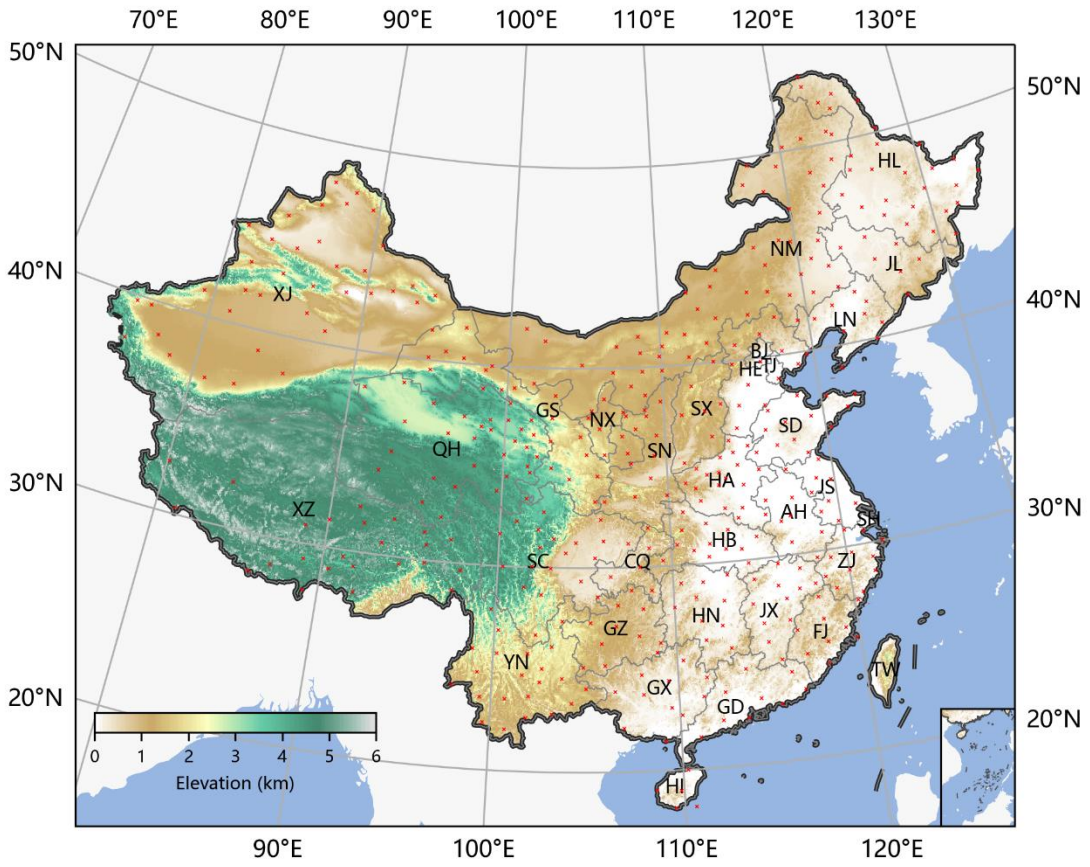

Fig. 1. CNLDN sites distribution and altitude distribution map of China with the location of each province and municipality (indicated by abbreviations, for details, refer to： *https://www.iso.org/obp/ui/#iso:code:3166:CN*）

3. CG flash characteristics of China

China's climate features are greatly influenced by its wide latitudinal span, significant terrain disparity, complex topography, and ocean currents (Ren et al., 2012). Lightning is a fundamental meteorological element, and its long-term accumulation characteristics are closely linked to China's climate. The spatial distribution of lightning in China is determined by a combination of factors, including atmospheric circulation, topography, distance from the sea, latitude, etc.

3.1 CG distribution in China

Previous studies have often divided China into four major geographical regions, each with relatively uniform climatic characteristics. These regions are Southern China (Region-I), Northern China (Region-II), Northwestern China (Region-III), and the Qinghai-Tibet region of China (Region-IV), as illustrated in Fig. 2. The Qinling Mountains-Huaihe River line, which roughly coincides with the 0 ℃ isotherm and 800 mm annual precipitation line in January, serves as the boundary between Region-I and

Region-II. The Daxing'an Mountains-Yinshan Mountains-Helan Mountains, which divide the monsoon and non-monsoon regions and the 400 mm annual precipitation line, serve as the boundaries between Region-II and Region-III. The boundary between Region-IV and Regions I-II-III is approximately the line between China's first and second steps in terrain.

Fig. 2 displays the distribution of annual average CG flash density from 2016-2021. Lightning primarily occurs in convective precipitation and, to a lesser extent, in stratus cloud precipitation. Generally, the spatial distribution of lightning is consistent with the distribution of annual average precipitation in China, as illustrated in Fig. 3 in Jin et al. (2021).

Region-I has the highest concentration of CG flashes, with a density greater than 1 km^{-2} yr^{-1}. The leap line of lightning density corresponds well with the 0 ℃ isotherms in January, the 800 mm annual equivalent precipitation line, and the eastern dividing line of the first and second terrain steps. The climate in Region-I is mainly influenced by the tropical/subtropical monsoon. The southeast monsoon from the Pacific Ocean and the southwest monsoon from the Indian Ocean make the summer hot and humid, and prone to thunderstorms. In particular, the monsoon influence is more pronounced in coastal areas with abundant water vapor and thermal conditions. In the mountainous regions of Hainan, Guangdong, Fujian, and Zhejiang, where the rolling topography lifts the warm and humid air masses, thunderstorm activity is most frequent, resulting in high lightning density. Although the Sichuan Basin and Yunnan are far from the coastline, they are located at the eastern and southern windward slopes of the Tibetan Plateau, which benefits the generation of thunderstorm activities due to the topographic uplift.

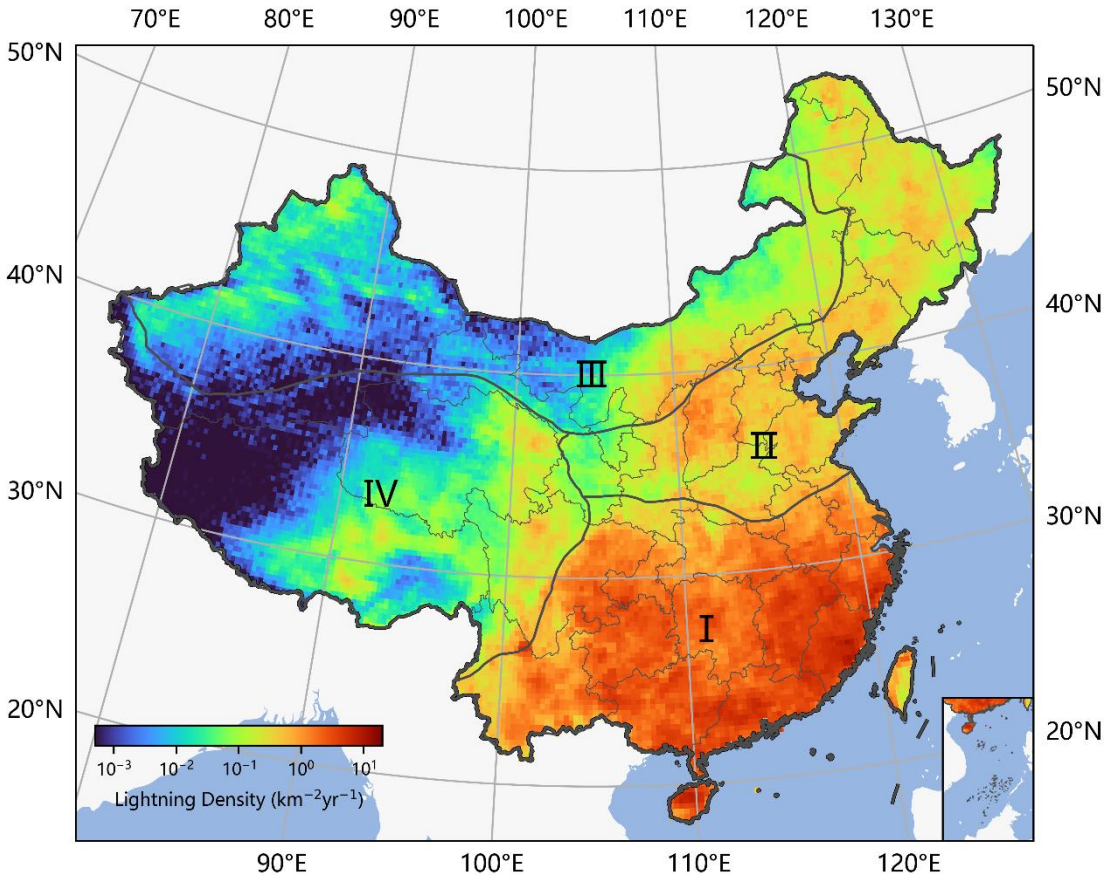

Fig. 2. 2016-2021 annual average CG flash density distribution in China. Region-I: Southern China; Region-II: Northern China; Region-III: Northwestern China; Region-IV: Qinghai-Tibet region of China. The gird size is 0.25° ×0.25°.

Region-II has a temperate monsoon climate, with summer influenced by the southeast monsoon carrying temperate marine air mass or degenerate tropical marine air mass, making summer warm and rainy. Most areas have CG flash density between 0.1-1 km^{-2} yr^{-1}, slightly lower than Region-I. The lightning density in Region-II is also greater in the seaside area than inland areas. Shanxi is located in a mountainous region, and the undulating terrain makes it a high incidence area for thunderstorm activity. Region-II has the most extensive plain, Northeastern China Plain, surrounded by the Daxing'an Mountains-Xiaoxing'an Mountains-Changbai Mountains. The landform is conducive to the southeast monsoon to reach the inland areas of Region-II and form summer thunderstorms. Jilin is only a dozen kilometers from the Sea of Japan, facilitating the entry of Japanese warm air currents. Therefore, despite its high latitude, thunderstorm activity is relatively intense in Region-II.

Region-III, which includes Xinjiang, northern Gansu, and most of Inner Mongolia, has a temperate continental climate. The southern and central parts of Region-III consist mostly of vast deserts and gobies. The Tibetan Plateau blocks the humid South Asian monsoon, and its arid surface cannot produce abundant water vapor, resulting in few thunderstorms. However, the Tianshan Mountains, Kunlun Mountains, Altay Mountains, and Tarbahatai Mountains located in the hinterland of the Eurasian

continent, are provided with water vapor for thunderstorm generation through the westerly circulation that transports evaporated water vapor from the Atlantic Ocean and the Eurasian continent. As a result, the northern mountainous areas occupy almost all the lightning activity in Xinjiang. The southeastern monsoon flowing through Region-II can also bring some thunderstorm processes to the eastern and central mountainous regions in Inner Mongolia during summer.

Region-IV's primary landmass is the Tibetan Plateau, which includes Tibet, Qinghai, southern Xinjiang, and western Sichuan. It has a highland mountain climate, and the overall geomorphic distribution trend increases from east to west (Ma et al., 2021). The uninhabited areas above 4500 meters in elevation in the west and north of Region-IV are icy all year round, covered by snow and glaciers. The Qaidam Basin in Qinghai is a closed, huge, interrupted basin, where dry sinking airflow from the northern edge of the plateau in summer leads to water shortage. Consequently, there are few thunderstorm activities in these areas, and the distribution of sub-stations is sparse, making them the regions with the lowest lightning density detected in China, with CG flash density less than 10^{-3} km^{-2} yr^{-1}. In contrast, the southern Himalayas, near the Yarlung Tsangpo River Grand Canyon, has a relatively low altitude, opening a "gap" for the influx of abundant water vapor from the Bay of Bengal. However, this narrow plain area, located in Mêdog County, has very high precipitation but low lightning density, which can also be concluded from the observations of TRMM. The remaining moisture continues northward across this plain, causing most thunderstorms between the east-west Himalayas Mountains and Tanggula Mountains. The thunderstorms on the east side of the plateau are mainly influenced by the low vortex and the shear line, which is usually stable at around 32.5°N(You et al., 2019; Qie et al., 2003). The high lightning density area is precisely located on the south side of the shear line.

3.2 Differences between +CG and -CG

Based on the different polarities of neutralized charges in thunderclouds, CG can be classified into two types: +CG and -CG. Generally, +CG has a lower occurrence probability, accounting for only about 10% of all CG, but it is characterized by a larger spatial scale and charge transfer, which results in a more significant hazard (Preston and Tolver, 1989; Carey and Buffalo, 2007). Studies have suggested that thunderstorms dominated by +CG are more likely to result in tornadoes and hail, particularly if the dominant phase lasts for tens of minutes. This may be related to changes in the charge distribution structure within thunderstorm clouds during extreme weather events(Williams, 1985). Previous research has been conducted on the comparative analysis of +CG and -CG in specific regions (Nag et al., 2014; Rakov and Uman, 2003). Based on these findings, this study aims to further investigate the spatial and temporal variability of +CG and -CG in China, taking into account the complex climatic and geographical factors that influence lightning activity.

3.2.1 Comparison of the temporal distribution of +CG and -CG

The geographical and climatic features differ considerably across the four regions. Therefore, we analyze the temporal distribution of lightning separately for each region.

Fig. 3 illustrates the monthly average CG flash frequency distribution in China over a six-year period from 2016 to 2021. The lightning frequency varies significantly across the four regions, with Region-I having the highest frequency, followed by Region-II and Region-III, and Region-IV having the lowest frequency. But the lightning frequency shows similar fluctuations throughout the year between the regions, with August having the highest frequency and December having the lowest. Lightning activity is also scarce in November, January, and February, with a sudden surge in March and a gradual increase in the following months. Based on the seasonal classification, lightning activity is most active in summer (June, July, and August), accounting for 70.7% of the year. In other seasons, lightning is more frequent in spring (19.1%) than in autumn (9.8%), but much less frequent than in summer. This is mainly because the summer monsoon affecting China starts to form during April and May, while the cold and dry winter monsoon starts to build up and push southward from September, making thunderstorm activity in spring and autumn mainly concentrated in southern areas, particularly coastal areas. In winter, most regions in China are controlled primarily by cold high pressure, resulting in very little lightning, with only a small amount occurring in southeastern coastal areas, accounting for just 0.4% of the year. Overall, lightning distribution follows a seasonal trend that advances from south to north and then retreats southward, which is consistent with the trend of the summer monsoon.

Furthermore, the proportion of +CG flashes in different months is calculated and represented by the gray line in Fig. 3. To ensure the reliability of the analysis, months with less than 50 +CG flashes are excluded to avoid the impact of outliers. Results indicate an evident inverse relationship between the proportion of +CG flashes and the frequency of lightning. Notably, the three months with the highest incidence of CG flashes, namely July, August, and September, exhibit the lowest proportion of +CG flashes across the four regions. During this period, Region-I and Region-IV, located at lower latitudes, exhibit a proportion of +CG flashes of approximately 0.1, while Region-II and Region-III display proportions of around 0.2. In other months, some irregular fluctuations are observed, among which Region-IV has rare thunderstorms in winter but demonstrates the highest proportion of +CG flashes, reaching 0.55. Moreover, Regions I and II show significantly high proportions of +CG flashes in February and April-May, respectively.

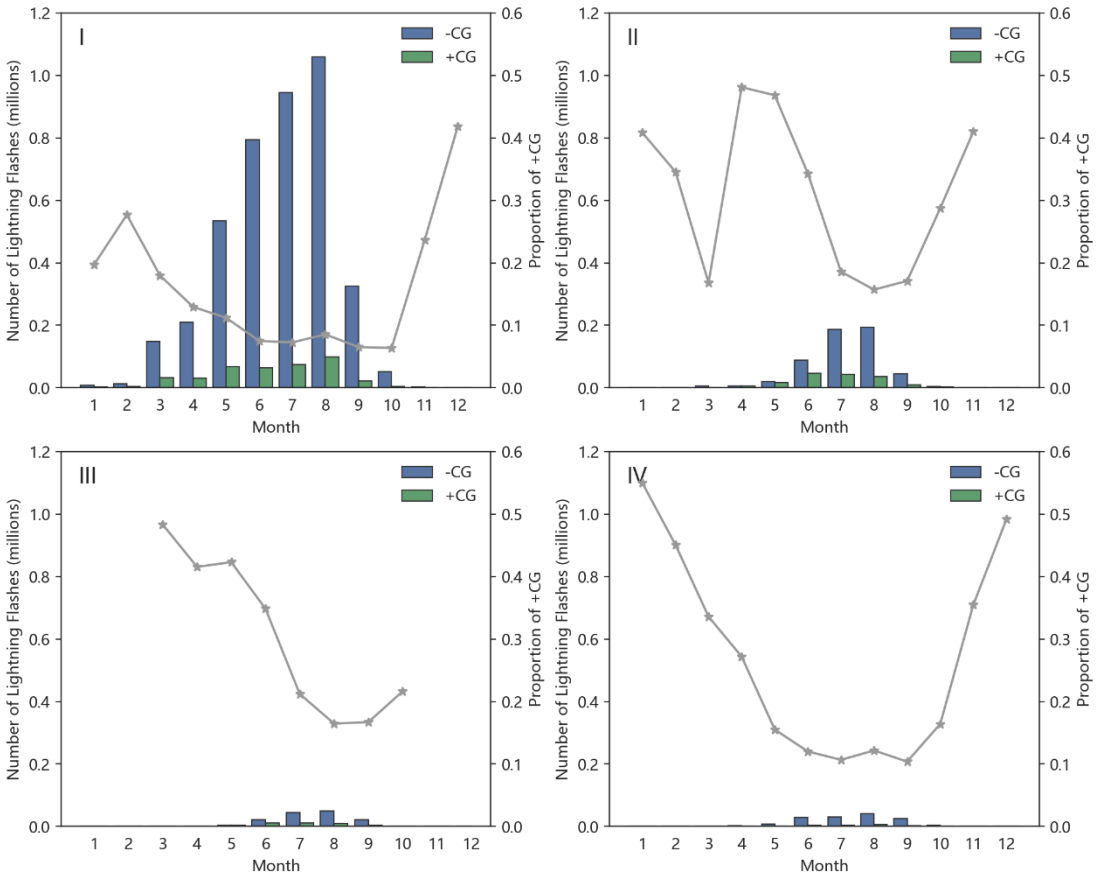

Fig. 3. Monthly variation of the frequency distribution of +CG and -CG flash. The gray line represents the proportion of +CG flash.

Fig. 4 illustrates the analysis of the current peak value of two types of CG flashes in different months and regions. To avoid outliers, no box is drawn when the flash count is less than 50. Overall, the distribution range is wider in winter than in other seasons, and Region-II has a wider current distribution interval than other regions. The average current peak value of each month is indicated by a white cross, and the variation trends are shown by red lines. The results indicate that +CG flashes generally have a higher discharge intensity than -CG flashes. The discharge intensity and the proportion of +CG flashes exhibit similar trends, with a higher proportion and stronger discharge intensity in winter and a lower proportion and weaker discharge intensity in summer. In Region-I and Region-II, the seasonal fluctuations of +CG current are more pronounced than -CG current, with the current of +CG falling even below -CG in August. The trends of +CG and -CG flash discharge intensity are more consistent in Regions-III and Region-IV.

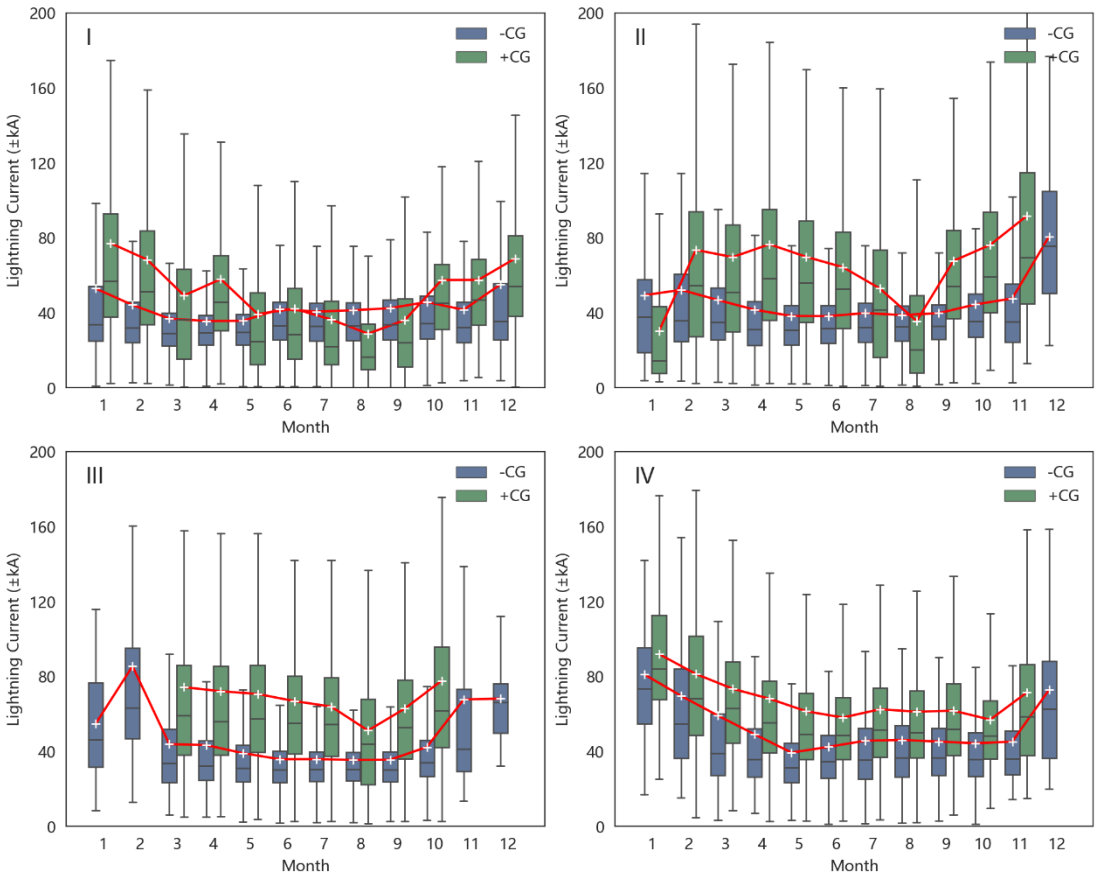

Fig. 4. Monthly variation of the peak current distribution of +CG and -CG flash. The red line represents the average peak current of each month. The -CG flash current is expressed in absolute value.

Fig. 5 illustrates the hour-by-hour frequency and intensity variations of CG flashes throughout the day. The frequency of both +CG and -CG flashes shows noticeable and consistent fluctuations. The active period for lightning activity is concentrated in the late afternoon to midnight, which coincides with the maximum accumulation of radiative heating and vapor conducive to the development of convection, particularly during summer thunderstorms in China. Lightning frequency peaks at 15:00 CNT (UTC+8) in Region-I and Region-II in the east of China and 1-2 hours later in Region-III and Region-IV in the west of China. After nightfall, lightning activity gradually weakens due to the decline in unstable energy, dropping to a trough at 8:00-10:00 CNT the following day.

The proportion of +CG flashes is inversely correlated with the total number of CG flashes in a day, as shown in Fig. 5. The maxima of the +CG proportion coincides with the lowest lightning frequency at 8:00-10:00 CNT in all four regions, but the minima appear 2-3 hours earlier than the frequency peak at 16:00 CNT. Region-I and Region-IV at low latitudes have maximum proportions in the morning, while Region-II and Region-III at high latitudes have maximum proportions in the evening. Additionally, the proportion of +CG flashes is lower in Region-I and Region-IV, with minimums of less than 0.1, than in Region-II and Region-III, where peak values can reach 0.3. These findings demonstrate a close relationship between thunderstorm characteristics and

geographical features such as latitude, topography, and sea distance.

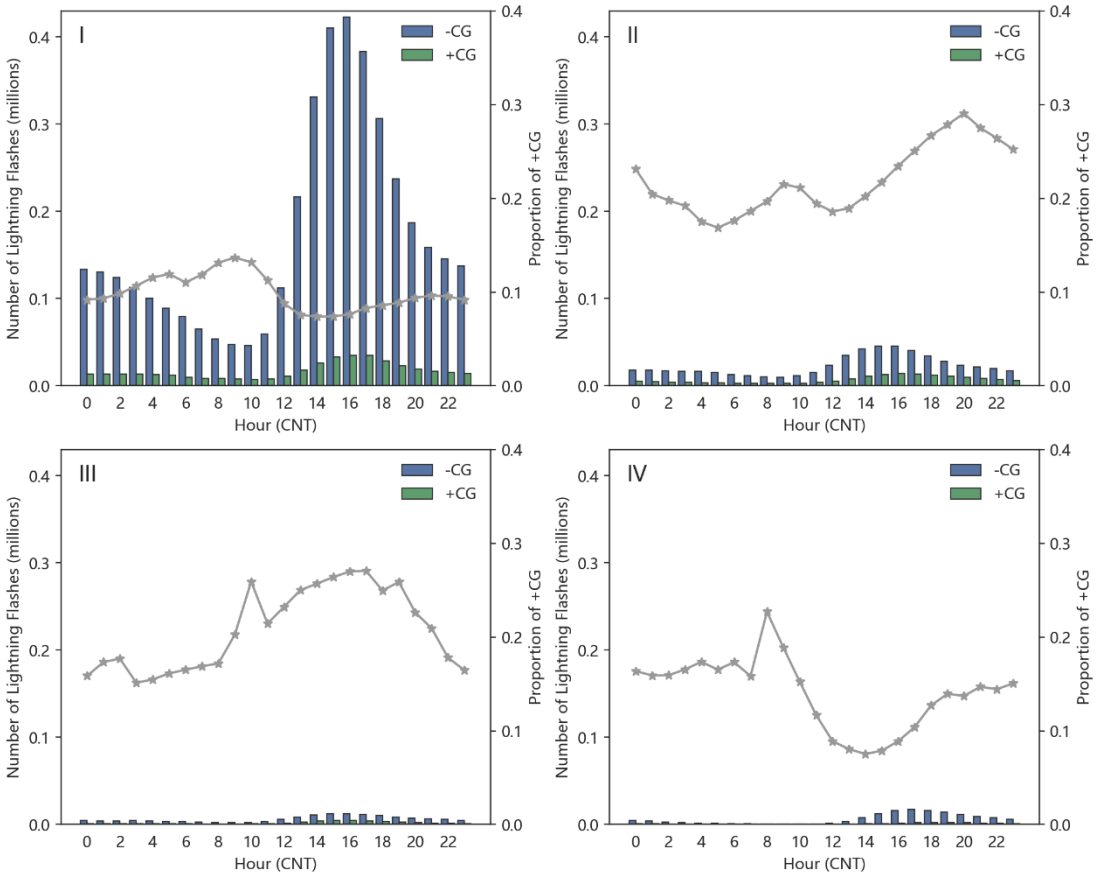

Fig. 5. Hourly variation of the frequency distribution of +CG and -CG flash. The gray line represents the proportion of +CG flash. The time zone is CNT (UTC+8).

The hourly current peak value distribution and their averages of +CG and -CG flashes are shown in Fig. 6. Region-II and Region-III, located at higher latitudes, have a wider distribution range of peak currents. But their variation is relatively stable, while the current of +CG in Region-III is slightly larger than in Region-II. The current in Region-1 decreases significantly in the noon and afternoon, with a more intense change in -CG than in +CG, resulting in the absolute current of two types of flashes even being reversed. Meanwhile, Region-IV, which has complex terrain due to the Qinghai-Tibet Plateau, exhibits intricate current variations, with an increase in +CG and a decrease in -CG. As a result, there is a huge disparity in current between the two types of flashes during noon and afternoon.

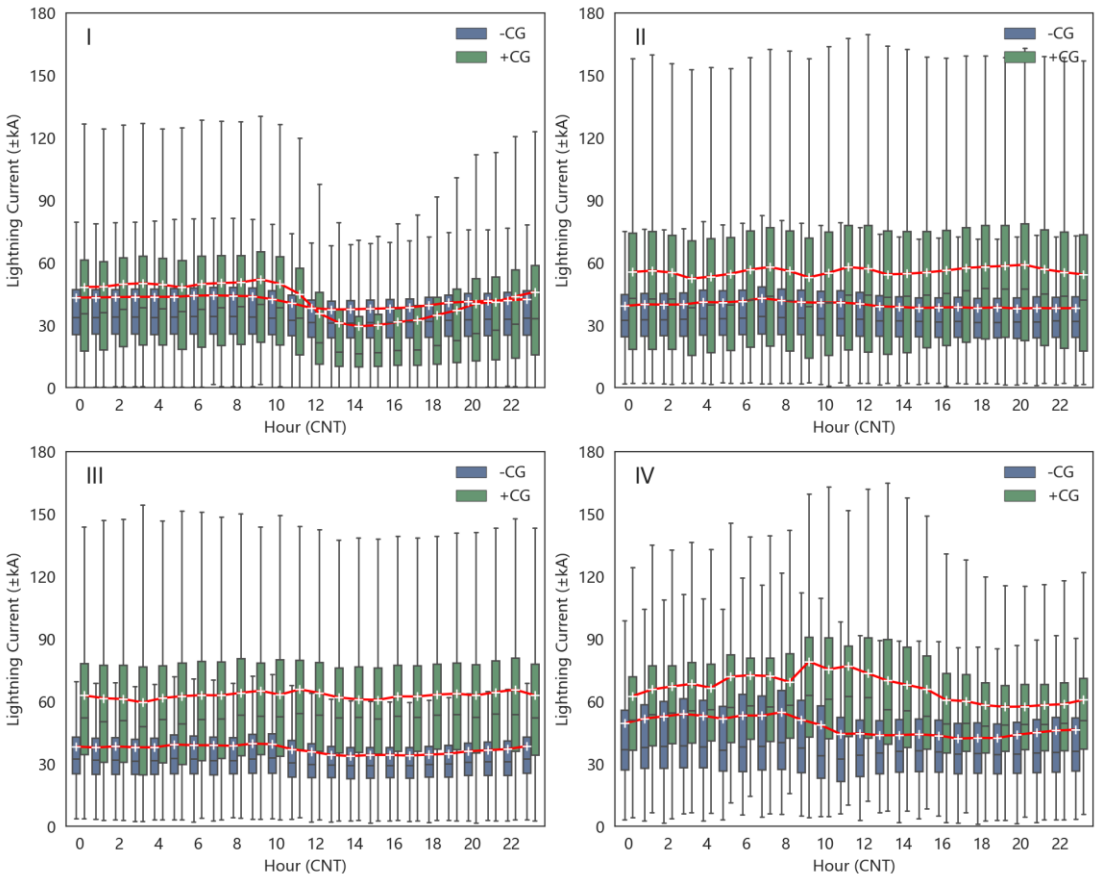

Fig. 6. Hourly variation of the peak current distribution of +CG and -CG flash. The red line represents the average peak current of each month. The -CG flash current is expressed in absolute value. The time zone is CNT (UTC+8).

3.2.2 Comparison of the spatial distribution of +CG and -CG

The geography of China is characterized by its complexity, and this is reflected in the variability of the ratio of +CG and -CG flashes across different regions. Fig. 7 illustrates the spatial distribution of the proportion of +CG flashes, with gray areas indicating grids with less than 50 CG flashes accumulated over a 6-year period. These grids are mainly located in the central, western, and northern parts of Tibet and the western and southern parts of Xinjiang. Region-I, which has the highest density of CG flashes, has a low proportion of +CG flashes, at less than 10%. Conversely, the other three regions have a higher proportion of +CG flashes, particularly the North China Plain and adjacent Inner Mongolia, as well as some parts of Region-III, where the +CG proportion can reach 30-40%. The proportion of +CG flashes in Shanxi and Shaanxi, both located in Region-II, is lower than in other regions of the same area. Overall, regions with lower CG flash density tend to have a higher proportion of +CG flashes, and high latitudes correspond to a higher +CG proportion.

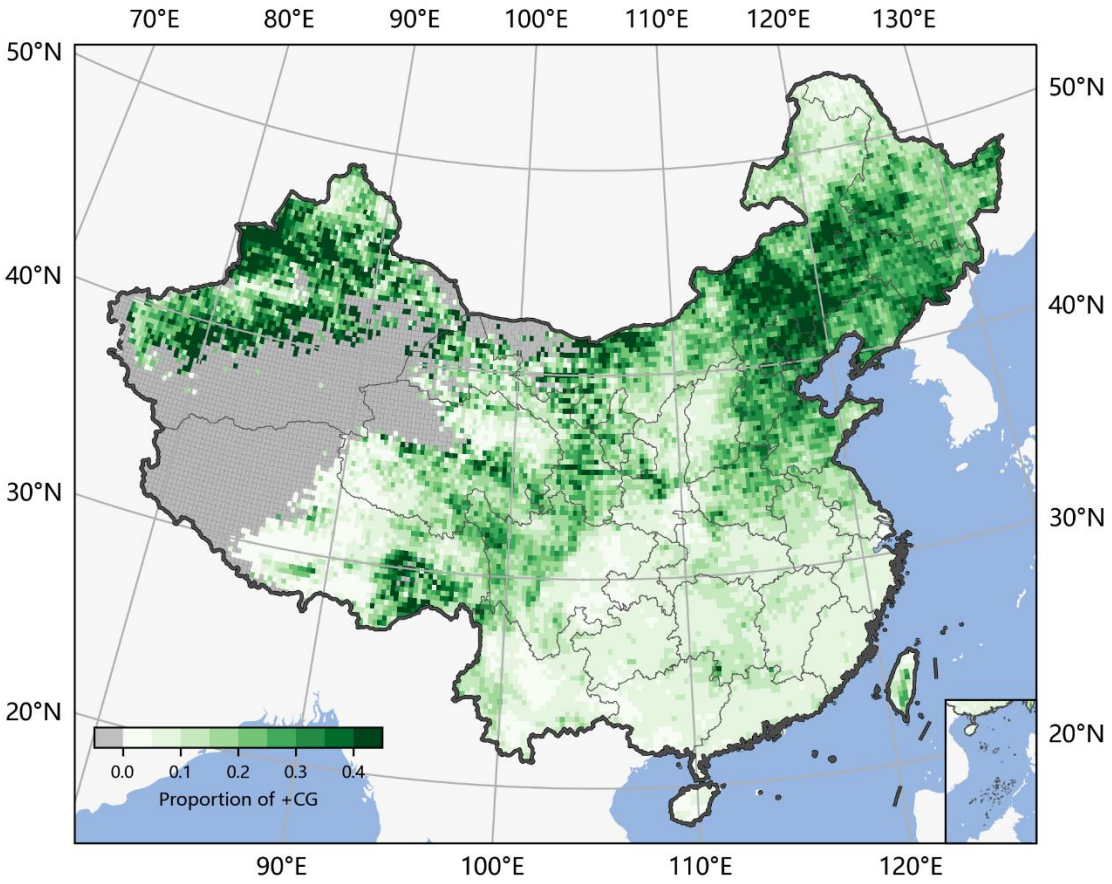

Fig. 7. Distribution of the proportion of +CG flashes in China. The gray grids have a CG flash number of less than 50 in 6 years and thus are not calculated. The gird size is 0.25° ×0.25°.

Based on Fig. 8, it can be inferred that the spatial distribution of the current values for both +CG and -CG is generally similar, with lower current values observed in the southeast, where lightning activity is more frequent, and higher current values found in other inland areas. Notably, the current values in southern Gansu, the plain in Mêdog County, and the intersection of Guizhou, Hunan, and Guangxi are higher, where the proportion of +CG is also relatively high. Therefore, it can be concluded that a high proportion of +CG typically corresponds to larger current values in terms of temporal and spatial scales.

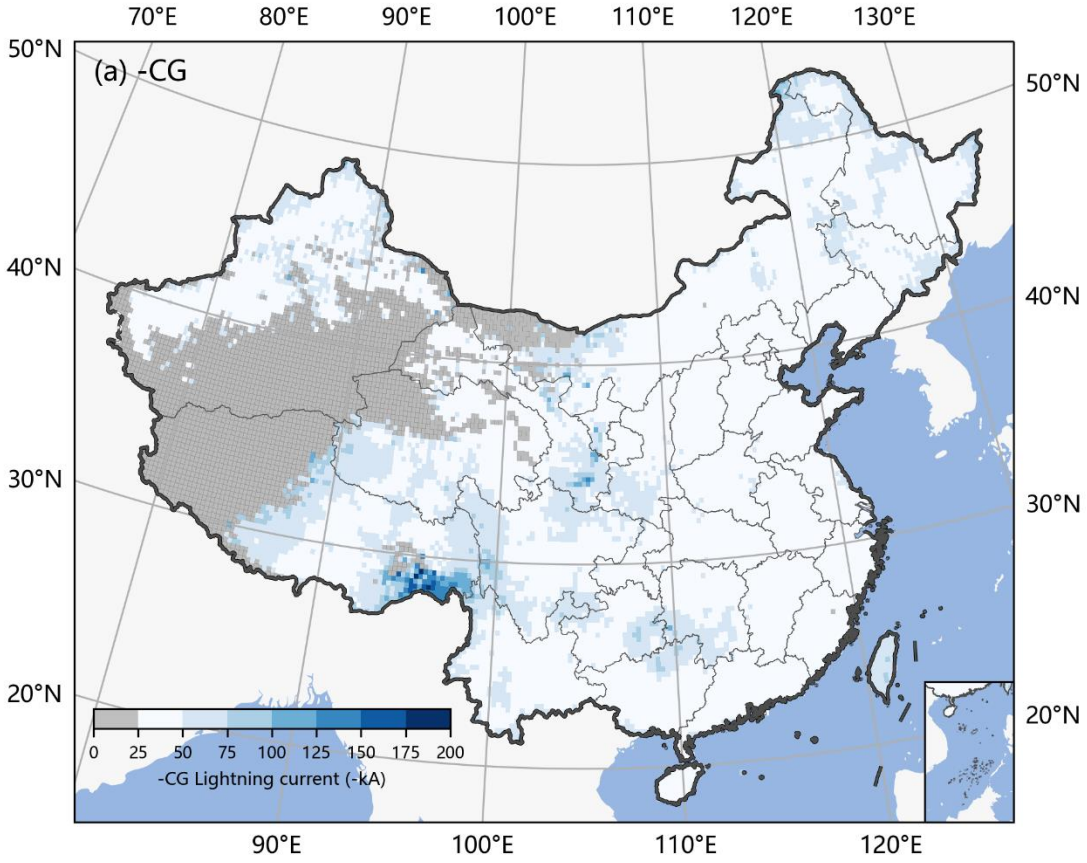
(a) -CG
70°E
80°E
90°E
100°E
110°E
120°E
130°E
50°N
40°N
30°N
20°N
0 25 50 75 100 125 150 175 200
-CG Lightning current (-kA)

330

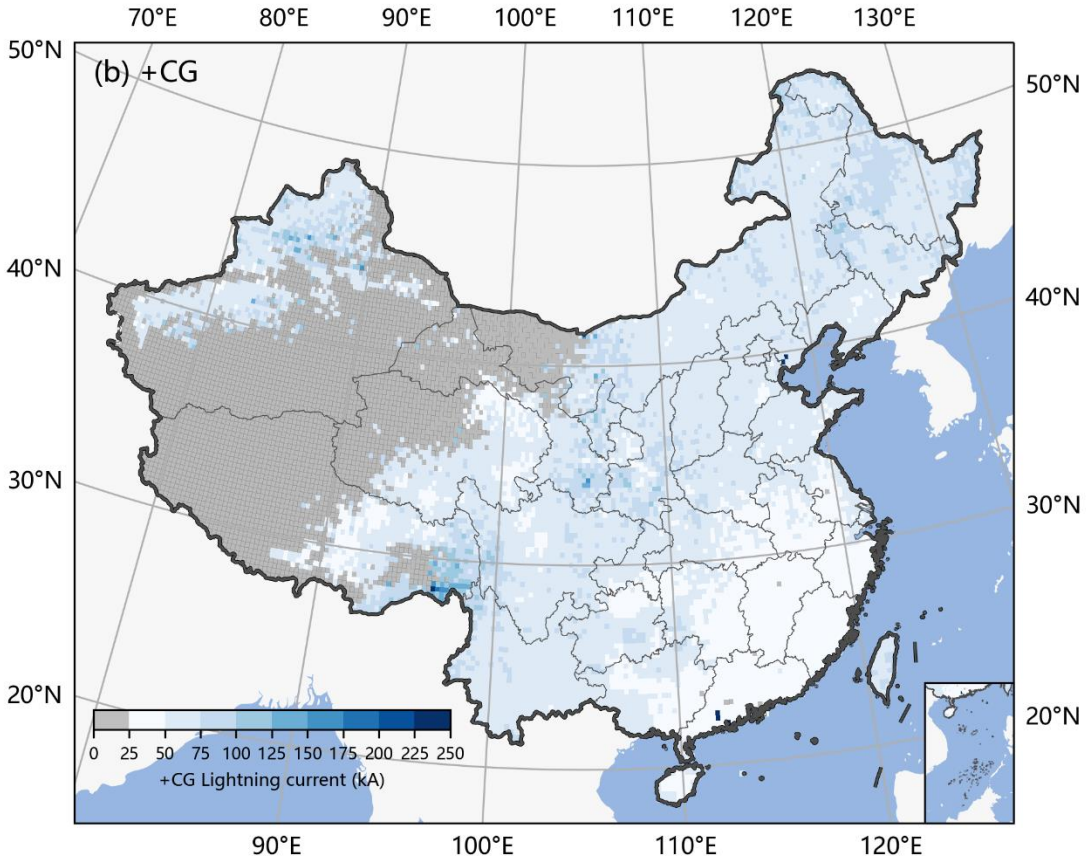
(b) +CG
70°E
80°E
90°E
100°E
110°E
120°E
130°E
50°N
40°N
30°N
20°N
0 25 50 75 100 125 150 175 200 225 250
+CG Lightning current (kA)

331

Fig. 8. Distribution of the average peak current of (a) -CG and (b) +CG flashes in China. The gray grids have a -CG or +CG flash number of less than 50 in 6 years and thus are not calculated. The gird size is 0.25° ×0.25°.

The proportion of +CG flashes in different altitude layers is calculated, as shown by the gray line in Fig. 9. Below 4500 meters altitude, the proportion increases with altitude, ranging from 7% to 15%. A sub-peak is observed at 1500 meters, which is caused by the high proportion region of +CG lightning flashes in Xinjiang and Inner Mongolia. However, above 4500 meters altitude, which mainly comprises the uninhabited areas of the western and northern Tibetan Plateau, the proportion of +CG lightning flashes decreases rapidly. It is worth noting that only 91 CG flashes occurred above 6000 meters of altitude during the six-year period and are not included in the statistics.

The box plot in Fig. 9 shows the current distribution of +CG and -CG lightning flashes at different altitudes. The distribution of lightning current decreases with increasing altitude. Interestingly, the average current of -CG lightning flashes shows a slight positive correlation with altitude, whereas +CG lightning flashes exhibit a negative correlation with altitude. The opposite trend of the two types of lightning flashes leads to a large difference in their discharge intensity at low altitudes and coincidence at high altitudes. Most of the reasons for the complexity of lightning activity in China come from the Tibetan Plateau, the "third pole" of the Earth, where the charge structure of thunderstorm clouds has some special characteristics due to the high-altitude ground surface(Li et al., 2013; Qie et al., 2005).

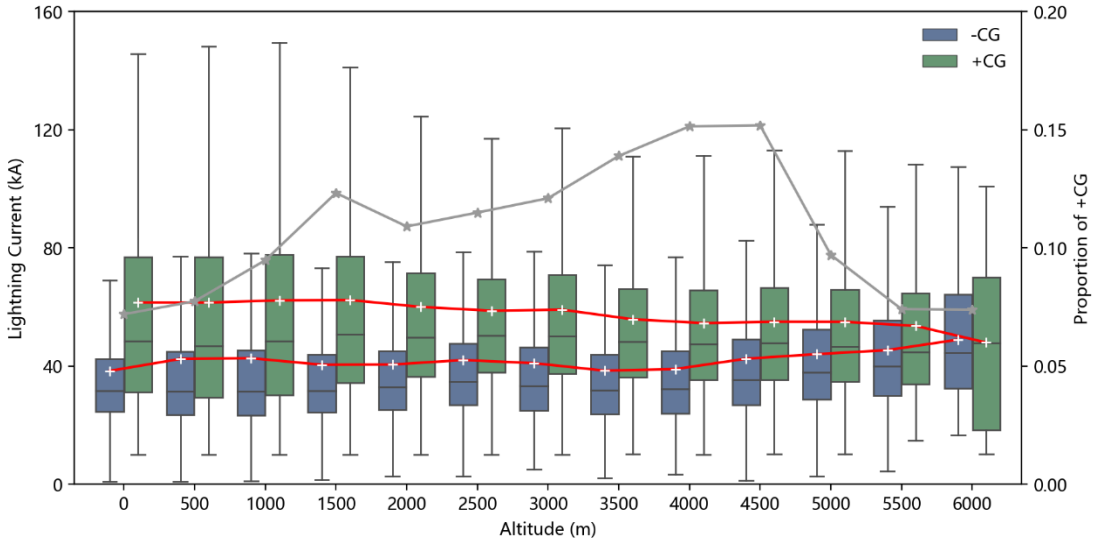

Fig. 9. The peak current distribution of +CG and -CG and the proportion of +CG versus altitude

4. Conclusion

China is primarily located in temperate and subtropical zones, with climate subject to a variety of factors, including cold and warm monsoons, the interplay of land and

sea, and varied topography. As a result, there are frequent convective weathers and a high prevalence of lightning activities. This paper utilizes the dataset from a ground-based lightning location system, CNLDN, which has relatively higher detection efficiency and smaller location errors for CG lightning compared with other national networks and the Lightning Mapping Imager on FY-4A satellite, to analyze the CG lightning characteristics in China over the past six years. The spatial and temporal distribution of +CG and -CG lightning exhibit regular patterns in terms of their frequency, ratio, and discharge intensity.

The results indicate that there are more CG lightning flashes in southern regions than in northern regions, more in mountainous areas than in plains at the same latitude, more in humid areas than in arid areas, and more in coastal areas than in inland areas within the same climate zone. The southeast coastland of China has the highest CG lightning density, while the northwest deserts and basins as well as the east and north Tibetan Plateau have the lowest density. The monsoon system plays a critical role in lightning activities in southern and Northern China, while the Tibetan Plateau contributes to the complexity of lightning activities in Northwestern China and the Qinghai-Tibet region. Overall, the distribution of lightning activity across China is consistent with the precipitation distribution observed at a climatic scale.

In general, +CG flashes have a lower occurrence rate than -CG flashes, but they carry higher currents and are more destructive. The spatial and temporal distribution of +CG and -CG flashes also varies significantly due to their different mechanisms. The lightning activity follows a seasonal pattern, with the highest frequency occurring during summer (70.7%), followed by spring (19.1%) and autumn (9.8%), and the least frequent in winter (0.4%). In spring, autumn, and winter, lightning is mainly concentrated in the southeastern coastal areas. The percentage of +CG flashes is inversely correlated with lightning frequency. High lightning frequency in summer generally corresponds to a low proportion of +CG flashes, while low frequency in winter corresponds to a high proportion of +CG flashes. The proportion of +CG flashes in winter thunderstorms in the eastern part of the Qinghai-Tibet Plateau is the highest, reaching up to 55%. The average discharge intensity of lightning is strongly correlated with the proportion of +CG flashes and also follows a seasonal pattern of being high in winter and low in summer. The seasonal fluctuations of +CG flashes are stronger than -CG flashes. In Southern China, the average intensity of +CG flashes in summer is even below -CG flashes. On the hourly scale, lightning is active in the late afternoon and midnight, with a peak between 15:00-17:00 CNT and drop to a trough the following day between 8:00-10:00 CNT. The proportion of +CG flashes throughout the day follows an inverse trend with the frequency of lightning, but the minimum proportion occurs 2-3 hours earlier than the maximum frequency. The highest proportion of +CG at low latitudes always occurs in the morning, while at high latitudes, it tends to occur at midnight. The changes in discharge intensity during the day at high latitudes are not significant. In Southern China, the discharge intensity of +CG and -CG flashes drops significantly at noon and afternoon, with +CG current dropping even lower than -CG

current.

The distribution of the +CG proportion exhibits significant spatial variability. In Southern China, where the density of CG lightning is the highest, the +CG proportion is the lowest, at less than 10%. In contrast, the high-latitude regions such as the North China Plain, Inner Mongolia, and northern and central Xinjiang have a much higher proportion of 30-40%. The proportion of +CG lightning below 4500 meters is positively correlated with altitude and drops sharply after exceeding 4500 meters in the western and northern regions of the Tibetan Plateau. The spatial distribution of discharge intensity of +CG and -CG is consistent, and a higher proportion of +CG lightning is generally associated with greater discharge intensity for both types. As latitude increases, the current distribution widens. The discharge intensity of +CG lightning shows a slight decrease with increasing altitude, while the intensity of -CG increases with altitude. Consequently, there is a significant difference in discharge intensities between the two types at low altitudes, but they tend to be similar at higher altitudes.

The lightning location system sites cannot be evenly distributed due to geographic factors, thus bringing about errors in lightning distribution analysis. The observation from the Lightning Mapping Imager (LMI) on the FY-4A satellite will be used to correct the distribution deviations by ground-based data in our following research. Given the vast size of China, a simple division into four regions may be too crude to study the influence of geographic and climatic factors on CG lightning characteristics in depth. Therefore, a more detailed division will be necessary for future studies.

Acknowledgments:

This study is supported by the Key Technologies Research and Development Program of China (2020YFB1600103). We appreciate the Meteorological Observation Centre of CMA and the Institute of Electrical Engineering of CAS for their data support. We also thank the reviewers and editors for their valuable suggestions for this study.

Reference

Carey, L. D. and Buffalo, K. M.: Environmental control of cloud-to-ground lightning polarity in severe storms, Monthly Weather Review, 135, 1327---1353, 2007.

Cummins, K. L., Murphy, M. J., Bardo, E. A., Hiscox, W. L., Pyle, R. B., and Pifer, A. E.: A combined TOA/MDF technology upgrade of the US National Lightning Detection Network, Journal of Geophysical Research: Atmospheres, 103, 9035-9044, 1998.

Jin, H., Chen, X., Wu, P., Song, C., and Xia, W.: Evaluation of spatial-temporal distribution of precipitation in mainland China by statistic and clustering methods, Atmospheric Research, 262, 105772, 2021.

Li, P., Zhai, G., Pang, W., Hui, W., Zhang, W., Chen, J., and Zhang, L.: Preliminary research on a comparison and evaluation of FY-4A LMI and ADTD data through a moving amplification matching algorithm, Remote Sensing, 13, 11, 2020.

Li, Y., Zhang, G., Wen, J., Wang, D., Wang, Y., Zhang, T., Fan, X., and Wu, B.: Electrical structure of a Qinghai–Tibet Plateau thunderstorm based on three-dimensional lightning mapping, Atmospheric Research, 134, 137-149, 2013.

Liu, Y., Wang, H., Li, Z., and Wang, Z.: A verification of the lightning detection data from FY-4A LMI as compared with ADTD-2, Atmospheric Research, 248, 105163, 2021.

Ma, M., Tao, S., Zhu, B., and Lü, W.: Climatological distribution of lightning density observed by satellites in China and its circumjacent regions, Science in China Series D: Earth Sciences, 48, 219-229, 2005.

Ma, R., Zheng, D., Zhang, Y., Yao, W., Zhang, W., and Cuomu, D.: Spatiotemporal Lightning Activity Detected by WWLLN over the Tibetan Plateau and Its Comparison with LIS Lightning, Journal of Atmospheric and Oceanic Technology, 38, 511-523, 2021.

Nag, A., Rakov, V. A., and Cummins, K. L.: Positive Lightning Peak Currents Reported by the U.S. National Lightning Detection Network, IEEE Transactions on Electromagnetic Compatibility, 56, 404-412, 2014.

Preston and Tolver, S.: The lightning discharge, Philosophical Magazine Series 1, 31, 443-445, 1989.

Qie, X., Toumi, R., and Zhou, Y.: Lightning activity on the central Tibetan Plateau and its response to convective available potential energy, Chinese Science Bulletin, 48, 296-299, 2003.

Qie, X., Zhang, T., Chen, C., Zhang, G., Zhang, T., and Wei, W.: The lower positive charge center and its effect on lightning discharges on the Tibetan Plateau, Geophysical research letters, 32, 2005.

Rakov, V. A. and Uman, M. A.: Lightning: Physics and Effects, Lightning: Physics and Effects2003.

Ren, G., Ding, Y., Zhao, Z., Zheng, J., Wu, T., Tang, G., and Xu, Y.: Recent progress in studies of climate change in China, Advances in Atmospheric Sciences, 29, 958-977, 2012.

Schulz, W., Diendorfer, G., Pedeboy, S., and Poelman, D. R.: The European lightning location system EUCLID–Part 1: Performance analysis and validation, Natural Hazards and Earth System Sciences, 16, 595-605, 2016.

Wang, J., Huang, Q., Ma, Q., Chang, S., He, J., Wang, H., Zhou, X., Xiao, F., and Gao, C.: Classification of VLF/LF Lightning Signals Using Sensors and Deep Learning Methods, Sensors (Basel, Switzerland), 20, 2020.

Williams, E. R.: Large‐scale charge separation in thunderclouds, Journal of Geophysical Research: Atmospheres, 90, 6013-6025, 1985.

You, J., Zheng, D., Zhang, Y., Yao, W., and Meng, Q.: Duration, spatial size and radiance of lightning flashes over the Asia-Pacific region based on TRMM/LIS observations, Atmospheric Research, 223, 98-113, 2019.